Mon. Not. R. astr. Soc. (1987) **227**, 161–183

The determination of the masses of Magellanic Cloud planetary nebulae using [O II] doublet ratio electron densities

M. J. Barlow★ *Joint Institute for Laboratory Astrophysics, University of Colorado and National Bureau of Standards, Boulder, CO 80309-0440, USA, and Department of Physics and Astronomy, University College London, Gower Street, London WC1E 6BT*

Accepted 1987 February 16. Received 1987 February 16; in original form 1986 September 29

Summary. Spectrophotometric data, including [O II] 3726, 3729 Å doublet ratios, are presented for 32 planetary nebulae (PN) in the Magellanic Clouds. It is argued that the electron densities derived from these ratios provide a much better diagnostic for the determination of nebular masses than previously assumed. The 32 PN are classified as either Type I or else as optically thick or optically thin in the hydrogen Lyman continuum. The optically thick PN are found to all have electron densities greater than 6000 cm^{-3}, while the optically thin PN all have electron densities below 5000 cm^{-3}. The optically thin PN show a range of only a factor of 2.0 in their derived masses, and have a mean ionized mass of $0.27 \pm 0.06\, M_{\odot}$. The absolute H$\beta$ fluxes of the optically thick nebulae show a range of only a factor of 1.8. The application of these results to Galactic PN would yield distances which are generally larger than those previously estimated. A method of distance determination is proposed for optically thin PN that uses integrated nebular [O II] electron densities rather than angular diameters.

1 Introduction

The masses of planetary nebula envelopes are of interest (i) because PN play a potentially important role in the enrichment of the interstellar medium in many heavy elements, (ii) because the nebular masses when combined with the masses of their central stars enable the masses of the immediate progenitor asymptotic giant branch stars to be related to those of the resulting white dwarfs, and (iii) because knowledge of PN envelope masses as a function of central star mass may enable constraints to be placed upon the PN formation mechanism.

In addition to these more global considerations, the determination of accurate nebular masses for a significant sample of PN is needed in order to test the validity of one of the most commonly used methods for the determination of distances to Galactic PN, namely the assumption that all optically thin PN have the same nebular mass (Shlovsky 1956). The number of Galactic PN with

★1985–86 JILA Visiting Fellow.

accurate independently determined distances is small and so several investigators have studied the systems of planetary nebulae in the Magellanic Clouds, for which more reliable distances are available. In a pioneering study, Webster (1969) obtained photoelectric fluxes for these nebulae for the first time and placed upper limits on their masses using angular diameter upper limits. Further progress on the determination of nebular masses by this method required the measurement of angular diameters, which for many Magellanic Cloud PN are expected to be of the order of 1 arcsec or less. Jacoby (1980), in a deep survey of PN in the SMC and LMC found several faint resolved nebulae with angular diameters of 2–3 arcsec, for which masses could be estimated. More recently, Barlow *et al.* (1986) and Wood, Bessell & Dopita (1986) have obtained speckle interferometry of brighter Magellanic Cloud PN, using the 3.9-m AAT, with the aim of determining nebular masses. The [O II] doublet ratio electron densities which are presented in this paper were originally obtained in order to supplement the analysis of further speckle data obtained at the AAT with the Imperial College Speckle Interferometer. However, it will be shown that the [O II] electron densities themselves allow useful estimates to be made of PN nebular masses.

Webster (1976) measured [O II] doublet ratios for four SMC PN from electronographic spectra and used the derived electron densities to estimate nebular masses. However, it has been argued, there and elsewhere, that densities derived from [O II] lines are unrepresentative of the overall nebulae, since they originate from a trace ionization stage. It will be shown in Section 3 that [O II] electron densities do in fact provide a reliable way of determining nebular masses, particularly for optically thin nebulae.

In Section 2 the spectrophotometric data are presented, while in Section 3 the theoretical justification for the use of forbidden-line densities for the determination of nebular masses is discussed. Section 4 discusses the determination of the extinction corrections that are needed for the observed Hβ fluxes, while the ionized nebular masses are derived in Section 5, along with predicted angular diameters, which are compared with existing angular diameter information. Section 6 includes an extensive discussion of the critieria used for the classification of the PN as either optically thick or optically thin in the hydrogen Lyman continuum. The derived nebular masses are discussed in Section 7, in the context of their implications for the viability of the Shlovsky method of distance determination.

In this paper the same nomenclature system for Magellanic Cloud PN will be adopted as is widely used for Galactic PN, i.e. the name and index number from the first discovery list. These are the lists of Henize (1956; SMC and LMC N), Lindsay (1961; SMC L), Lindsay & Mullan (1963; LMC LM) and Jacoby (1980; SMC J). A cross-index of names is available in the catalogue of Sanduleak, MacConnell & Philip (1978).

2 Observations

The spectra were acquired with the IPCS and RGO Spectrograph 25-cm camera on the 3.9-m AAT, using a 1200 lines mm^{-1} grating in first order to give a spectral dispersion of 33 Å mm^{-1}. Two-dimensional spectra were obtained, each with between 20 and 40 spatial increments of 2.3 arcsec per increment. The slit widths used for the observations ranged between 0.6 and 1.8 arcsec, yielding resolutions of between 1.1 and 1.6 Å, as judged from the FWHMs of comparison arc lines. The seeing during the observations ranged between 1.5 and 2.5 arcsec. Table 1 presents the journal of observations. The 1985 spectra were acquired during PATT AAT service time. All of the spectra included the 3500–4200 Å region, although the total wavelength coverage varied slightly from night to night, so that some spectra included the Hγ and [O III] 4363 Å lines, while others did not. The notation 'n.o.' in Table 2(a) and (b) indicate when these lines did not fall within the observed wavelength range.

Table 1. Journal of observations.

Date	Name	Slit-width (arcsecs)	Exposure time (seconds)
November 22/23 1978	SMC J2	1.8	1600
July 6/7 1979	SMC N6	1.5	560
"	SMC N8	"	300
"	SMC N87	"	350
"	SMC L302	"	440
"	LMC N97	"	250
"	LMC N28	"	240
"	LMC N110	"	200
"	LMC N203	"	310
"	LMC N141	"	200
January 4/5 1985	SMC N2	1.4	600
"	SMC N5	"	300
"	SMC N43	"	600
"	SMC N54	"	1000
"	SMC N38	"	500
"	SMC N40	"	800
"	SMC N44	"	500
"	SMC N67	"	700
"	LMC N184	"	250
"	LMC N102	"	300
"	LMC N133	"	450
"	LMC N201	"	250
"	LMC N66	"	300
"	LMC LM1-61	"	400
May 17/18 1985	SMC N4	0.6	1200
"	SMC L66	0.6	400
September 4/5 1985	SMC L536	0.8	300
"	SMC L239	"	"
"	SMC N70	"	"
"	SMC L305	"	"
"	LMC N122	"	"
"	LMC N153	"	"
"	LMC N178	"	"

The data were reduced using the SDRSYS, SPICA and IRAF packages. The spatial increments containing the sky background* were summed and weighted and subtracted from the central increments containing the object spectra. Wavelength calibration was obtained by means of fifth-order polynomial fits to the positions of 30–40 Cu–Ar comparison arc lines spread over the observed wavelength range, and relative flux calibration was obtained by means of observations of white dwarf stars from the list of Oke (1974). The PN emission-line fluxes were determined mainly using the DIPSO package (Howarth & Maslen 1984) at the UCL STARLINK node, although the final nights data were analysed using the IRAF package (Shames & Tody 1986) on the JILA VAX 8600. In order to maximize the accuracy of the relative intensities derived for the slightly blended [O II] 3726 and 3729 Å lines, the DIPSO Gaussian fitting routine, ELF, written by Dr

*SMC L66 was found to be situated in a region of low surface brightness nebular emission, the [O II] doublet ratio of this emission being at the low-density limit. This background is probably due to outlying emission from the bright H II region SMC N13 (=NGC 248), which is located about 1 arcmin north of L66.

Table 2. (a) Observed relative line intensities.

λ(Å)	Ion	SMC N2	SMC N4	SMC N5	SMC N6	SMC L66	SMC N38	SMC N40	SMC N43
3722	H14+[S III]		3.2		2.6		2.3		2.1
3726	[O II]	17.4	8.2	45.1	7.8	43.9	12.7	18.4	8.8
3729	[O II]	10.3	5.5	24.2	2.9	52.2	5.8	10.3	3.8
3734	H13		2.0		1.8		2.0		
3750	H12		3.0	3.1	2.0		3.8		
3760	O III	3.4	2.2						
3771	H11		3.8	4.7	3.4	3.1	3.5	3.8	3.5
3798	H10	6.5	5.5	4.8	4.0	5.8	4.6	5.1	5.8
3820	He I		1.3		1.1				1.1
3835	H9	8.7	5.9	8.2	6.3	10.1	5.9	7.1	7.0
3868	[Ne III]	70.1	37.4	75.1	59.0	61.1	49.8	66.1	39.3
3889	H8+He I	20.0	20.6	22.4	14.4	16.6	15.9	17.8	14.9
3967	[Ne III]	19.7	12.5	19.6	17.9	25.3	13.6	17.9	12.4
3970	H7	16.4	14.8	13.9	12.3	15.1	15.8	14.4	15.0
4026	He I + He II	3.2	2.3	2.1	1.8		2.4		2.6
4068	[S II]	2.7	1.1	3.3	1.6		1.8	4.3	
4097	N III								
4101	Hδ	25.2	25.6	25.2	21.8	25.1	25.4	25.4	25.6
4227	[Fe V]								
4267	C II		1.3			1.9	1.5		0.7
4340	Hγ	47.5	45.8	41.9	n.o.	52.6	45.5	42.7	45.9
4363	[O III]	n.o.	9.4	n.o.	n.o.	14.2	n.o.	n.o.	n.o.

λ(Å)	Ion	SMC N44	SMC L239	SMC N54	SMC L302	SMC L305	SMC N67	SMC N70	SMC N87
3722	H14+[S III]	2.4	1.6	2.0		3.4		3.4	2.4
3726	[O II]	13.5	19.7	3.2	354.	20.4	34.1	56.1	11.7
3729	[O II]	6.8	10.5	1.1	300.	7.1	17.8	23.8	5.3
3734	H13	2.3		2.4					2.5
3750	H12	3.2	2.8	3.2					3.0
3760	O III					10.4			
3771	H11	3.4	3.1	3.5				4.8	3.8
3798	H10	6.1	5.3	4.0	5.7		7.6	6.1	5.2
3820	He I	1.8		1.2					1.5
3835	H9	6.9	9.6	7.2	7.5	8.3	6.6	8.7	7.2
3868	[Ne III]	64.6	65.9	18.9		76.7	43.9	24.5	32.7
3889	H8+He I	18.7	16.9	12.3	23.8	27.7	22.7	18.4	19.7
3967	[Ne III]	17.5	15.1	5.7		18.4	11.6	6.2	9.7
3970	H7	14.6	13.6	13.8	16.2	15.5	15.1	15.3	14.3
4026	He I + He II	2.0	1.6	2.1		5.1		2.6	1.9
4068	[S II]		2.1		3.1	4.0	5.5	1.2	0.3
4097	N III								
4101	Hδ	25.1	24.8	25.7	24.9	24.6	24.9	24.8	25.6
4227	[Fe V]					3.6	2.9		
4267	C II	1.6		0.7				0.5	
4340	Hγ	43.2	42.5	41.5	n.o.	42.0	45.0	43.5	n.o.
4363	[O III]	n.o.	12.2	n.o.	n.o.	19.9	n.o.	3.9	n.o.

P. J. Storey, was used. The derived flux ratios, $I(3726)/I(3729)$ are listed in column 9 of Table 5. Fig. 1 show examples of the [O II] doublet at the high-density limit (LMC N110, typical of the signal-to-noise obtained on most of the spectra) and at the low-density limit (SMC J2, by far the faintest PN in the sample).

Although the observed wavelength range did not include Hβ, the relative line fluxes were put on to the usual scale relative to Hβ=100 by first dereddening all fluxes with a Galactic reddening law (Howarth 1983), using the extinctions listed in column 4 of Table 5, and then normalizing the dereddened relative fluxes to Hδ=26.1, the theoretical case B intensity relative to Hβ=100 for $T_e=1.3\times10^4$ K and $n_e=1.0\times10^4$ cm^{-3} (Brocklehurst 1971). The resulting dereddened relative

Table 2 (a) *continued*

λ(Å)	Ion	SMC L536	SMC N8	LMC N184	LMC N97	LMC N102	LMC N28	LMC N110	LMC N122
3722	H14+[S III]			3.0	3.3	3.6	2.2	1.9	5.2
3726	[O II]	16.6	182.	50.0	66.0	40.4	39.2	37.5	29.8
3729	[O II]	11.6	198.	26.9	40.7	17.3	17.5	13.1	18.4
3734	H13					1.8		1.3	
3750	H12			2.8		2.2		2.3	
3760	O III			2.2	2.0	4.1	2.5		2.3
3771	H11	3.7		2.1	2.0	3.9		3.2	3.4
3798	H10	4.9	3.5	4.8	3.6	4.0	2.7	4.5	4.6
3820	He I			1.3	1.2	1.2		0.8	1.1
3835	H9	8.8	4.7	5.6	4.4	5.2	5.1	6.4	7.1
3868	[Ne III]	65.0	1.8	90.1	117.2	124.3	76.4	97.6	124.2
3889	H8+He I	27.2	9.1	15.2	18.9	18.4	12.4	17.1	17.3
3967	[Ne III]	10.8		25.7	35.9	36.3	30.2	30.4	34.1
3970	H7	16.1	11.5	12.7	11.2	12.2	10.9	13.6	14.6
4026	He I + He II	4.1		0.8	2.5	2.5	1.3	2.1	1.7
4068	[S II]	4.7		2.5	0.9	9.5	3.6	2.6	6.3
4097	N III					1.2	1.3		1.5
4101	Hδ	25.6	20.6	24.3	24.2	24.4	23.5	24.3	24.3
4227	[Fe V]								
4267	C II			0.5					
4340	Hγ	48.3	n.o.	39.9	n.o.	45.6	n.o.	n.o.	46.5
4363	[O III]	13.1	n.o.	n.o.	n.o.	n.o.	n.o.	n.o.	19.3

λ(Å)	Ion	LMC N133	LMC N201	LMC N141	LMC N203	LMC N153	LMC N66	LMC N178	LMC LM1-61
3722	H14+[S III]	2.6	3.3	1.8	2.2	2.3	5.2	2.1	1.9
3726	[O II]	4.7	22.7	22.6	49.5	34.4	34.9	29.9	12.8
3729	[O II]	1.6	11.1	10.1	18.3	17.8	20.8	16.0	8.5
3734	H13	1.7	1.6	1.8	1.9			2.0	1.7
3750	H12	2.2	2.4	2.9	2.3		3.2	2.2	2.8
3760	O III		2.8			2.8	3.5	1.8	3.0
3771	H11	3.3	3.3	3.1	3.5	4.2	3.6	3.3	
3798	H10	3.7	4.3	4.3	4.0	4.6	4.8	4.2	5.9
3820	He I	1.7	1.7	0.8	0.6	0.9	2.2		
3835	H9	5.3	5.9	6.6	5.8	6.9	8.2	7.0	7.5
3868	[Ne III]	36.3	82.4	64.5	38.4	91.8	107.7	91.4	59.3
3889	H8+He I	12.6	16.0	16.8	17.4	15.7	20.0	15.9	16.6
3967	[Ne III]	10.6	26.3	19.7	11.2	28.1	32.2	24.0	17.1
3970	H7	14.3	14.5	15.8	14.1	14.3	17.8	12.4	13.9
4026	He I + He II	1.5	1.7	2.1	1.7	2.9	2.9	2.1	
4068	[S II]	1.2	3.1	0.8	1.6	3.7	4.3	2.8	
4097	N III		0.5		0.5				1.0
4101	Hδ	24.4	24.0	24.6	24.3	24.3	25.1	23.9	24.8
4227	[Fe V]		2.0				2.5		
4267	C II	1.1	0.3					0.6	
4340	Hγ	40.1	40.1	n.o.	n.o.	43.2	46.7	42.0	44.0
4363	[O III]	n.o.	n.o.	n.o.	n.o.	17.8	n.o.	15.9	n.o.

line fluxes are listed in Table 2(b). The observed relative line fluxes are given in Table 2(a), again relative to Hβ=100. Table 3 presents a comparison between the dereddened and theoretical line intensities, relative to Hβ, for seven Balmer lines. The mean Balmer line intensities show satisfactory agreement with the theoretical intensities. The one standard deviation limits (column 4) indicate that errors of ±20 per cent can be associated with line strengths weaker than 8.0, while the errors for lines with strengths greater than 15.0 are less than 10 per cent. The accuracy of the *ratio* of $I(3726)/I(3729)$, determined separately with the Gaussian fitting routine, is estimated to be better than ±0.08 in all cases.

Table 2. (b) Dereddened relative line intensities.

λ(Å)	Ion	SMC N2	SMC N4	SMC N5	SMC N6	SMC L66	SMC N38	SMC N40	SMC N43
3722	H14+[S III]		3.3		3.3		2.4		2.2
3726	[O II]	18.2	8.5	47.3	10.1	46.3	13.2	19.1	9.0
3729	[O II]	10.8	5.7	25.4	3.8	55.1	6.0	10.7	3.9
3734	H13		2.0		2.3		2.1		
3750	H12		3.1	3.2	2.5		4.0		
3760	O III	3.5	2.2						
3771	H11		3.9	4.9	4.4	3.2	3.6	3.9	3.6
3798	H10	6.8	5.7	5.0	5.1	6.1	4.8	5.3	6.0
3820	He I		1.3		1.4				1.1
3835	H9	9.1	6.1	8.6	7.9	10.6	6.1	7.4	7.2
3868	[Ne III]	73.1	38.5	78.4	74.2	64.1	51.7	68.6	40.4
3889	H8+He I	20.8	21.2	23.3	18.0	17.4	16.5	18.4	15.3
3967	[Ne III]	20.5	12.8	20.4	22.0	26.4	14.0	18.5	12.7
3970	H7	17.0	15.1	14.5	15.1	15.8	16.3	14.9	15.4
4026	He I + He II	3.3	2.3	2.2	2.2		2.5		2.7
4068	[S II]	2.8	1.1	3.4	1.9		1.9	4.4	
4097	N III								
4101	Hδ	26.1	26.1	26.1	26.1	26.1	26.1	26.1	26.1
4227	[Fe V]								
4267	C II		1.3			2.0	1.5		0.7
4340	Hγ	48.6	46.4	42.9	n.o.	53.9	46.4	43.6	46.6
4363	[O III]	n.o.	9.5	n.o.	n.o.	14.6	n.o.	n.o.	n.o.

λ(Å)	Ion	SMC N44	SMC L239	SMC N54	SMC L302	SMC L305	SMC N67	SMC N70	SMC N87
3722	H14+[S III]	2.5	1.8	2.1		3.7		3.6	2.5
3726	[O II]	14.2	21.2	3.3	378.	22.2	36.3	60.1	12.0
3729	[O II]	7.2	11.2	1.1	320.	7.7	19.0	25.5	5.5
3734	H13	2.4		2.5					2.6
3750	H12	3.3	3.0	3.3					3.1
3760	O III					11.3			
3771	H11	3.5	3.4	3.6				5.2	3.9
3798	H10	6.5	5.7	5.1	6.1		8.0	6.5	5.4
3820	He I	1.9		1.2					1.6
3835	H9	7.3	10.3	7.3	7.9	8.9	7.0	10.6	7.4
3868	[Ne III]	67.8	70.2	19.3		82.6	46.5	26.1	33.6
3889	H8+He I	19.6	18.0	12.6	25.2	29.8	24.0	19.6	20.2
3967	[Ne III]	18.3	16.0	5.8		19.7	12.2	6.6	9.9
3970	H7	15.2	14.4	14.1	17.1	16.5	15.9	16.2	14.6
4026	He I + He II	2.1	1.7	2.2		5.4		2.8	2.0
4068	[S II]		2.2		3.3	4.3	5.8	1.3	0.3
4097	N III								
4101	Hδ	26.1	26.1	26.1	26.1	26.1	26.1	26.1	26.1
4227	[Fe V]					3.8	3.1		
4267	C II	1.6		0.7				0.5	
4340	Hγ	44.4	44.0	42.0	n.o.	43.7	46.5	45.0	n.o.
4363	[O III]	n.o.	12.6	n.o.	n.o.	20.7	n.o.	4.0	n.o.

3 The derivation of nebular masses using densities from forbidden-line ratios

The mass of a fully ionized nebula is given by

$$M(\text{ion}) = \mu m_{\text{H}} \int_0^{\infty} \varepsilon n_{\text{H}}(r) 4\pi r^2 \, dr, \tag{1}$$

where $n_{\text{H}}(r)$ is the hydrogen density distribution as a function of radius r, ε is the nebular filling factor, m_{H} is the mass of a hydrogen atom and μ, the mean ionic mass per H-atom, is given by $\mu = (1+4y)$, where $y = n(\text{He})/n(\text{H})$.

Table 2 (b) *continued*

λ(Å)	Ion	SMC L536	SMC N8	LMC N184	LMC N97	LMC N102	LMC N28	LMC N110	LMC N122
3722	H14+[S III]			3.3	3.73	3.9	2.6	2.1	5.7
3726	[O II]	17.1	253.	55.2	73.4	44.0	45.5	41.5	33.0
3729	[O II]	11.9	275.	29.7	45.2	19.4	20.3	14.5	20.3
3734	H13				2.8	2.0		1.5	
3750	H12			3.1	3.1	2.4		2.5	
3760	O III			2.4	2.2	4.5	2.9		2.5
3771	H11	3.8		2.3	2.2	4.3		3.5	3.7
3798	H10	5.0	4.8	5.3	4.0	4.4	3.1	4.9	5.0
3820	He I			1.5	1.4	1.3		0.8	1.2
3835	H9	9.0	6.4	6.1	4.8	5.7	5.8	7.0	7.8
3868	[Ne III]	66.7	2.4	98.6	128.9	135.4	87.3	106.8	135.9
3889	H8+He I	27.9	12.2	16.6	20.7	20.0	14.1	18.7	18.9
3967	[Ne III]	11.1		27.9	39.2	39.3	34.1	33.1	37.1
3970	H7	16.5	15.0	13.8	12.3	13.2	12.3	14.8	15.9
4026	He I + He II	4.2		0.8	2.7	2.7	1.5	2.3	1.8
4068	[S II]	4.8		2.7	9.6	10.2	4.0	2.8	6.8
4097	N III					1.2	1.4		1.6
4101	Hδ	26.1	26.1	26.1	26.1	26.1	26.1	26.1	26.1
4227	[Fe V]								
4267	C II			0.6					
4340	Hγ	49.0	n.o.	41.9	n.o.	47.7	n.o.	n.o.	48.8
4363	[O III]	13.3	n.o.	n.o.	n.o.	n.o.	n.o.	n.o.	20.3

λ(Å)	Ion	LMC N133	LMC N201	LMC N141	LMC N203	LMC N153	LMC N66	LMC N178	LMC LM1-61
3722	H14+[S III]	2.9	3.8	2.0	2.4	2.5	5.5	2.4	2.0
3726	[O II]	5.2	26.2	24.5	54.7	38.0	36.8	33.9	13.7
3729	[O II]	1.8	12.8	10.9	20.2	19.7	21.9	18.1	9.1
3734	H13	1.9	1.8	2.0	2.1			2.2	1.8
3750	H12	2.4	2.8	3.2	2.5		3.4	2.5	3.0
3760	O III		3.2			3.1	3.7	2.0	3.2
3771	H11	3.6	3.8	3.4	3.9	4.6	3.8	3.7	
3798	H10	4.1	4.9	4.6	4.4	5.0	5.0	4.7	6.3
3820	He I	1.9	1.9	0.8	0.6	1.0	2.3		
3835	H9	5.7	6.7	7.1	6.4	7.5	8.6	7.8	8.0
3868	[Ne III]	39.5	92.3	69.5	42.0	100.5	113.0	102.2	63.2
3889	H8+He I	13.7	18.1	18.0	19.0	17.2	21.0	17.8	17.7
3967	[Ne III]	11.4	29.4	21.1	12.2	30.5	33.6	26.6	18.1
3970	H7	15.5	16.2	16.9	15.3	15.5	18.6	13.7	14.7
4026	He I + He II	1.7	1.8	2.3	1.9	3.1	3.0	2.3	
4068	[S II]	1.2	3.4	0.8	1.7	4.0	4.4	3.1	
4097	N III		0.5		0.5				1.0
4101	Hδ	26.1	26.1	26.1	26.1	26.1	26.1	26.1	26.1
4227	[Fe V]		2.2				2.6		
4267	C II	1.1						0.6	
4340	Hγ	42.0	42.6	n.o.	n.o.	45.4	47.9	44.7	45.5
4363	[O III]	n.o.	n.o.	n.o.	n.o.	18.7	n.o.	16.9	n.o.

The dereddened Hβ flux received from the nebula is given by

$$I(\mathrm{H}\beta)=\frac{\alpha_{\mathrm{eff}}(\mathrm{H}\beta)h\nu_\beta}{4\pi D^2}\int_0^\infty \varepsilon n_{\mathrm{e}}(r)n_{\mathrm{H}}(r)4\pi r^2\,dr, \tag{2}$$

where $\alpha_{\mathrm{eff}}(\mathrm{H}\beta)$ is the effective recombination coefficient of hydrogen for the emission of Hβ photons of energy $h\nu_\beta$, and D is the distance of the nebula. From equations (1) and (2) one obtains

$$M(\mathrm{ion})=\frac{4\pi D^2 I(\mathrm{H}\beta)(1+4y)m_{\mathrm{H}}}{\alpha_{\mathrm{eff}}(\mathrm{H}\beta)h\nu_\beta\langle n_{\mathrm{e}}\rangle} \tag{3}$$

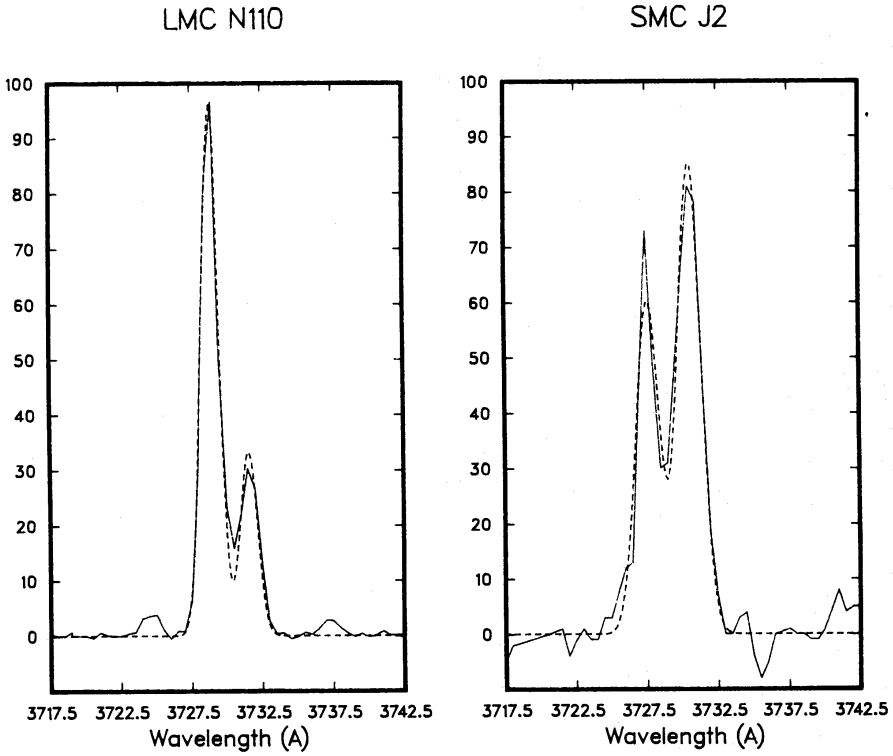

Figure 1. Examples of the fits to the [O II] doublet profiles, for LMC N110 (left) and SMC J2 (right). The solid curves are the observed profiles, while the dashed curves are the fits. The Gaussians fitted to each of the doublet components were constrained to have identical halfwidths, the halfwidth being allowed to vary from object to object. The ordinate for SMC J2 is detected photons per increment, while the ordinate for the higher signal-to-noise spectrum of LMC N110 is normalized flux.

Table 3. Mean dereddened Balmer line intensities, relative to Hβ=100.

λ(Å)	Transition	Number of data points	Mean ±1σ	Case B theory ($n_e = 10^4$ cm^{-3} $T_e = 10^4$ K)*
3734	H13	15	2.13 ± 0.34	2.44
3750	H12	19	2.97 ± 0.42	3.09
3771	H11	25	3.75 ± 0.65	4.00
3798	H10	31	5.28 ± 0.95	5.33
3835	H9	32	7.60 ± 1.57	7.34
3970	H7	32	15.3 ± 1.36	15.9
4340	Hγ	23	45.6 ± 2.9	46.9

*From Brocklehurst (1971).

where

$$\langle n_e \rangle = \frac{\int_0^\infty \varepsilon n_e(r) n_H(r) r^2 \, dr}{\int_0^\infty \varepsilon n_H(r) r^2 \, dr}. \quad (4)$$

Substituting from Brocklehurst (1971) for $\alpha_{eff}(H\beta)$ at $n_e = 10^4\,cm^{-3}$ and $T_e = 10^4$–2×10^4 K, one

obtains

$$M(\text{ion}) = \frac{8.12\times10^{11} I(\text{H}\beta) t^{0.913}(1+4y) D^2(\text{kpc})}{\langle n_e \rangle} M_\odot, \tag{5}$$

where $t = T_e/10^4\,\text{K}$.

The intensity ratio of the $^2D^0_{3/2,\,5/2} - {}^4S^0_{3/2}$ 3726 and 3729 Å transitions of [O II] is an electron density diagnostic. For the upper levels i of each of these transitions, one can define (Osterbrock 1974) the critical density $n_c(i)$ as

$$n_c(i) = \frac{\sum_{j<i} A_{ij}}{\sum_{j\neq i} q_{ij}}, \tag{6}$$

where A_{ij} are the downwards transition probabilities and q_{ij} are the upwards and downwards collisional rates from the level. For $n_e \ll n_c(i)$, radiative de-excitations of the upper level dominate collisional rates out of the level, while for $n_e \gg n_c(i)$ collisions will dominate. With the collision strengths of Pradhan (1976) and the transition probabilities of Zeippen (1982), one finds

$n_c(^2D^0_{3/2}) = 4160$ and $5340\,\text{cm}^{-3}$ for $T_e = 10^4\,\text{K}$ and $2\times10^4\,\text{K}$;

$n_c(^2D^0_{5/2}) = 940$ and $1160\,\text{cm}^{-3}$ for $T_e = 10^4\,\text{K}$ and $2\times10^4\,\text{K}$.

At densities significantly below the critical density, the collisional excitation rates and radiative de-excitation rates will be in balance, and proportional to $n_e n(\text{ion})$, while at densities significantly above the critical density a Boltzmann population distribution will be established and the radiative de-excitation rate will be proportional to $n(\text{ion})$ only. Thus, for $1000\,\text{cm}^{-3} \lesssim n_e \lesssim 5000\,\text{cm}^{-3}$, we have

$$\frac{I(3726)}{I(3729)} \propto \frac{\int_0^\infty \varepsilon n_{O^+}(r) n_e(r) r^2\,dr}{\int_0^\infty \varepsilon n_{O^+}(r) r^2\,dr}. \tag{7}$$

For a low-excitation nebula in which O^+ is the dominant ionization stage of oxygen (e.g. SMC L302), one obtains $n_{O^+}(r) \propto n_H(r)$ and so the ratio on the right-hand side of relation (7) is the same as that defining the mean nebular electron density $\langle n_e \rangle$, in equation (4). However, in most planetary nebulae O^{2+} is the dominant ionization stage of oxygen (the coincidence of the ionization potentials of O^{2+} and He^+ ensures that this is the case, even in high-excitation PN). In such nebulae the density of O^+ is determined by the balance between recombinations of O^{2+} and photo-ionizations of O^+ by the r^{-2} diluted stellar radiation field. Thus

$$n_{O^+}(r) \propto n_{O^{2+}}(r) n_e(r) r^2 \propto n_H(r) n_e(r) r^2. \tag{8}$$

Substituting for $n_{O^+}(r)$ into equation (7), one obtains

$$\frac{I(3726)}{I(3729)} \propto \frac{\int_0^\infty \varepsilon n_e^2(r) n_H(r) r^4\,dr}{\int_0^\infty \varepsilon n_e(r) n_H(r) r^4\,dr} \equiv \langle n_e' \rangle. \tag{9}$$

For the case of a uniform density, or an r^{-2} density distribution, $\langle n_e \rangle$ and $\langle n_e' \rangle$ are identical.

Harrington & Feibelman (1983) have shown that the observed brightness distributions of PN can be fitted by combinations of Gaussian density distributions. Consider first the case of a density distribution which can be represented by a single Gaussian

$$n_e(r)=N_O \exp\left[-\left(\frac{r-r_O}{\sigma_O}\right)^2\right]^{1/2}. \quad (10)$$

In addition, one has $n_H(r)=n_e(r)/\gamma$, where γ is the mean number of electrons per proton. Substituting from (10), equation (4) can be evaluated to obtain

$$\langle n_e\rangle = \frac{N_O \exp(r_O/\sigma_O)}{8}. \quad (11)$$

One can also substitute from equation (10) into (9) to obtain

$$\langle n_e'\rangle = \frac{N_O \exp(r_O/\sigma_O)}{7.6}. \quad (12)$$

Therefore the electron density $\langle n_e'\rangle$ defined by the [O II] 3726, 3729 Å doublet ratio should differ by only 5 per cent from the mean nebular electron density $\langle n_e\rangle$ defined by equations (3) and (4), provided $1000\,\mathrm{cm}^{-3} \lesssim n_e \lesssim 5000\,\mathrm{cm}^{-3}$. The same result is found to hold for nebulae with density distributions that can be represented by a superimposition of multiple Gaussians.

Low surface-brightness high-excitation planetary nebulae which have He II 4686 Å stronger than Hβ are likely to be optically thin in both the He II and H I continua (see the discussion, for a Galactic sample, by Kaler 1981). For these nebulae, O^{3+} is likely to be the dominant ionization stage of oxygen, so that relationship (8) will not apply. However, such nebulae, which are spectroscopically easy to recognize, are not included in the present sample (and are likely to have undetectable [O II] 3727 Å fluxes in most cases).

The utility, as a nebular mass tracer, of the electron density derived from the [O II] 3726, 3729 Å

Table 4. Masses of model nebulae versus masses derived from predicted [O II] and C III] doublet ratios.

PN name	NGC 7662	IC 3568	NGC 3918	SMC N2
reference	1	2	3	4
$L_*(L_\odot)$	6100	1100	6900	4340
T_{eff}(K)	120,000	50,000	140,000	110,000
D(kpc)	1.5	1.0	1.5	57.5
Model log I(Hβ) (cgs)	-9.761	-10.572	-9.635	-12.686
Model T_e(O III) (K)	12,140	10,600	12,500	13,500
Model (1+4y)	1.376	1.396	1.428	1.436
Model n_e(O II) cm^{-3}	3060	4540	2400	2900
Model n_e(C III) cm^{-3}	4220	7910	4610	3720
Model M(PN) ($M_\odot$)	0.20	7.26×10^{-3}	0.26	0.356
M(O II) ($M_\odot$)	0.170	7.06×10^{-3}	0.309	0.360
M(O II) error	18%	3%	16%	1%
M(C III) ($M_\odot$)	0.123	4.05×10^{-3}	0.161	0.281
M(C III) error	62%	79%	61%	28%

References: (1) Model II of Harrington et al. (1982); (2) Model A2 of Harrington and Feibelman (1983); (3) Clegg et al. (1986); (4) Barlow et al (1986).

ratio can be confirmed by considering the results obtained from theoretical nebular modelling. Detailed ionization structure models have been constructed in the last few years for three PN: NGC 7662 (Harrington *et al.* 1982), IC 3568 (Harrington & Feibelman 1983) and NGC 3918 (Clegg *et al.* 1987). Table 4 summarizes some of the basic parameters of these models. It also includes the parameters from the less comprehensive modelling of SMC N2 (Barlow *et al.* 1986). Each model predicted an integrated flux ratio $I(3726)/I(3729)$, which I have evaluated with the multi-level statistical equilibrium code EQUIB in order to derive the corresponding electron density, n_e(O II). This evaluation was carried out for the O III electron temperature, T_e(O III), predicted by each model. Nebular masses M(O II) were then derived by substituting n_e(O II) in place of $\langle n_e \rangle$ in equation (5), using $t = T_e(\text{O III})/10^4\,\text{K}$. The resulting values of M(O II) can be compared with the true model nebular masses M(PN), also listed in Table 4. The error in the M(O II) mass, defined as $[M(\text{PN}) - M(\text{O II})]/M(\text{O II})$, is tabulated, in percentage terms, in the row following M(O II).

The models for NGC 7662, IC 3568 and SMC N2 are all optically thin in the hydrogen Lyman continuum, and the derived values of M(O II) agree to within 18, 3 and 1 per cent, respectively, with the value of M(PN) (the model for SMC N2 was specifically constructed to match the [O II] ratio and [O III] ratio). In the model for NGC 3918 (Clegg *et al.* 1987), 53 per cent of the mass resides in optically thick sectors, in which a thin outer region with $n(\text{O II}) > n(\text{O III})$ would exist. However, the derived value of M(O II) for NGC 3918 differs by only 16 per cent M(PN), again a tolerable error.

Also listed in Table 4 are the electron densities, n_e(C III), that are derived from the predicted ratio of the integrated fluxes in the C III] 1907 and 1909 Å lines, for each model. It can be seen that the nebular masses M(C III), derived using n_e(C III) in equation (5), show poor agreement with the model nebular masses M(PN), the smallest error being 28 per cent and the largest 79 per cent. The reason for this is that the critical densities for the upper levels of both of the C III transitions are significantly above the range of electron densities encountered in most PN ($n_e \sim 8\times10^4\,\text{cm}^{-3}$ for $^3P_2$ and $\sim 1\times10^9\,\text{cm}^{-3}$ for $^3P_1$, at $T_e = 10^4\,\text{K}$). The C III] 1907 to 1909 Å ratio therefore provides a measure of n_e which is weighted to higher densities and which is less suitable as a mass tracer, than that provided by the [O II] 3726, 3729 Å doublet ratio. So, despite the fact that C^{2+} is a much more abundant ion in most PN than O^+, electron densities from [O II] are more appropriate for the derivation of nebular masses using equation (5).

The $^2P^0_{3/2,\,1/2}$ levels of [O II], which give rise to the 7320, 7330 Å multiplet, have critical densities of $n_c \sim 5\times10^6\,\text{cm}^{-3}$ at $T_e = 10^4\,\text{K}$. Therefore when nebular electron densities significantly exceed $n_e \sim 5\times10^3\,\text{cm}^{-3}$, the ratio $I(7325)/I(3727)$, rather than $I(3726)/I(3729)$, will be proportional to the right-hand side of relation (9), and thus the electron density derived from $I(7325)/I(3727)$ can be used as a mass tracer when the $I(3726)/I(3729)$ ratio is no longer useful (however, the [O II] 7325 Å flux must first be corrected for the contribution by O^{2+} dielectronic recombination – see Rubin 1986).

One may also consider whether any density-sensitive line ratios from other ions might be suitable as nebular mass tracers. The critical densities, at $T_e = 10^4\,\text{K}$, quoted below, utilize the atomic data compiled by Mendoza (1983). The 6717 and 6731 Å transitions of [S II] provide a commonly used nebular density diagnostic, their upper levels having critical densities of 1170 and $4330\,\text{cm}^{-3}$, respectively. However, S^{3+}, rather than S^{2+}, is often the dominant ionization stage of sulphur in PN, so that the density of S^+ cannot be linked to the local number density in the simple fashion that the O^+ density can [relation (8)]. Densities derived from [S II] line ratios may thus provide a less reliable measure of $\langle n_e \rangle$ for use in equation (5) than those derived from [O II] line ratios.

Accurate collision cross-sections for [Cl III] and [Ar IV] will soon be available (K. Butler, private communication), thereby enabling their use as reliable density diagnostics. However, the

abundances of Cl^{2+} and Ar^{3+} are likely to show a more complicated dependence upon nebular parameters than is the case for O^+ and O^{2+}, thus restricting their use as mass tracers.

Amongst the density-sensitive infared fine structure line ratios, it is clear that the [O III] ^3P fine structure lines at 88 and 52 μm would make very good nebular mass tracers for intermediate-density nebulae, since (i) the critical densities for the $^3P_1$ and $^3P_2$ levels are 680 and 3470 cm^{-3}, respectively, and (ii) O^{2+} is the dominant stage of oxygen in most PN and in many H II regions. For lower density H II regions, in which either N^+ or N^{2+} is the dominant ionization stage of nitrogen, the ratio of the [N II] ^3P fine structure lines at 204 and 122 μm will provide a useful mass tracer density diagnostic, since the critical densities of the [N II] $^3P_1$ and $^3P_2$ levels are 60 and 270 cm^{-3}, respectively.

4 Hβ fluxes and extinctions for Magellanic Cloud PN

Column 2 of Table 5 lists the observed Hβ flux $F(H\beta)$, for each nebula, adopted from the sources listed in column 3. Large-aperture Hβ fluxes are available for most of the nebulae. However, four of the SMC PN only have narrow-slit flux estimates available at present (relative to PN with known fluxes): the Hβ fluxes for these four nebulae are listed in parentheses to indicate lower reliability.

Column 4 of Table 5 lists the extinction of Hβ, $C(H\beta)$, that was adopted for each nebula in order to derive the dereddened Hβ flux, $I(H\beta)$, listed in column 5. At present, most of the PN in the sample lack reliable spectrophotometric estimates for extinction: radio fluxes are not available for use in the radio–Hβ method, while the relatively short-wavelength baseline between Hα and Hβ necessitates a high degree of spectrophotometric accuracy when estimating extinctions from observed Hα/Hβ ratios. Therefore the extinctions of most of the PN in the sample have been estimated by the following method: (i) The values of $C(H\beta)$ labelled 'Galaxy' in Table 5 are based upon the Galactic reddening maps of Burstein & Heiles (1982), and I have adopted $C(H\beta)=1.45E(B-V)$, from the Galactic optical reddening function of Howarth (1983). (ii) The values of $C(H\beta)$ labelled 'SMC' in Table 5(a) were obtained from the map of N(H I) for the SMC published by Hindman (1967; via his fig. 2), applying Fitzpatrick's (1985) determination of $N(H\,I)/E(B-V)=8.7\times10^{22}\,cm^{-2}\,mag^{-1}$ for the SMC and the assumption that $C(H\beta)=1.45E(B-V)/2$ (i.e. that each PN is located halfway along the SMC dust column at its position). (iii) The $C(H\beta)$ estimates labelled 'LMC' in Table 5(b) were obtained from the N(H I) table of Rohlfs *et al.* (1984), with the adoption of $N(H\,I)/E(B-V)=2\times10^{22}\,cm^{-2}\,mag^{-1}$ for the LMC (Koornneef 1982), again assuming that $C(H\beta)=1.45\,E(B-V)/2$.

The extinction derived for SMC N2 by this method is in agreement with the value derived from the observed ratio of He II 1640 Å to He II 4686 Å (Barlow *et al.* 1986). Estimates of $C(H\beta)$ from He II 1640 to 4686 Å ratios are also available for four LMC PN (Barlow *et al.*, in preparation). The derived extinctions confirm that N66 lies about half-way along its LMC dust column, while N97, N28 and N201 are at the rear of their respective LMC dust columns. In Table 5(b), for these four PN the estimates derived from their He II flux ratios have been adopted. Finally, optical spectrophotometry of SMC N6 and N8 has shown that they undergo significant extinction, with $C(H\beta)=0.43$ and 0.56, respectively (Barlow & Adams, in preparation). These values are adopted in Table 5(a). It is possible that a few other PN in the present sample undergo significant small-scale structure reddening, in which case their dereddened Hβ fluxes and derived nebular masses will be underestimated.

5 Derivation of ionized nebular masses for Magellanic Cloud PN

Equation (5) has been used to derive the ionized masses of the planetary nebulae in our sample. Distances of 57.5 and 47 kpc were adopted for the SMC and LMC, respectively, corresponding to

Table 5. (a) Derived nebular parameters for SMC PN.

(1) Name	(2) log F(Hβ) (cgs)	(3) Source for (2)	(4) C(Hβ) Galaxy	(4) C(Hβ) SMC	(5) log I(Hβ) (cgs)	(6) (1+4y)	(7) t	(8) Source for (6) and (7)	(9) $\frac{I(3726)}{I(3729)}$	(10) n_e (cm^{-3})	(11) M(ion) ($M_\odot$)	(12) Optically thick or thin	(13) Predicted ang. diam (arc sec)
SMC N2	-12.78	4	0.07	0.01	-12.69	1.43	1.34	9	1.69	2850	0.36	Thin	0.89
SMC N4	(-13.21)	8	0.03	0.02	(-13.16)	1.43	1.20	6	1.46	1780	0.18	Thin	0.81
SMC N5	-12.86	3	0.06	0.02	-12.78	1.45	1.36	9	1.86	3890	0.22	Thin	0.68
SMC N6	-12.82	1	0.03	0.40	-12.39	1.44	1.35	7	2.65	2.6×10^4	0.080	Thick	0.26
SMC J2	-14.83	11	0.03	0.06	-14.74	(1.5)	(1.25)	11	0.68	50; see text	0.19	(Type I)	2.8 obs.
SMC L66	(-13.85)	8	0.03	0.06	(-13.76)	1.44	1.23	6	0.84	270	0.30	Thin	1.84
SMC N38	-12.49	3	0.03	0.04	-12.42	1.35	1.28	6	2.20	7230	0.24	Thick	0.58
SMC N40	-12.89	1	0.03	0.04	-12.82	1.36	1.23	6	1.79	3300	0.20	Thin	0.71
SMC N43	-12.44	3	0.03	0.02	-12.39	1.44	1.20	9	2.30	8780	0.21	Thick	0.51
SMC N44	-12.54	3	0.09	0.00	-12.45	1.42	1.21	9	1.98	4620	0.35	Thin	0.75
SMC L239	(-12.93)	8	0.06	0.06	(-12.81)	1.50	1.27	6	1.88	3920	0.20	Thin	0.65
SMC N54	-12.42	4	0.04	0.00	-12.38	1.44	1.21	9	2.91	7.4×10^4	0.023	Thick	0.12
SMC L302	-13.34	7	0.09	0.02	-13.23	(1.43)	1.1	7	1.18	930	0.27	Thin	1.12
SMC L305	-13.04	3	0.09	0.05	-12.90	1.54	(1.8)	6	2.87	(4×10^4)	0.022	Type I	(0.14)
SMC N67	-12.88	4	0.09	0.02	-12.77	1.74	2.6	4,10	1.91	4240	0.45	Type I	0.82
SMC N70	-12.72	3	0.09	0.03	-12.60	1.39	1.10	9	2.36	9800	0.10	Thick	0.39
SMC N87	-12.48	3	0.03	0.02	-12.43	1.43	1.15	7	2.16	6410	0.25	Thick	0.60
SMC L536	(-13.23)	6,8	0.04	0.01	(-13.18)	1.91	2.5	6	1.43	1940	0.40	Type I	1.00
SMC N8*	-13.25	7	0.04	0.52	-12.69	(1.4)	(1.0)	7	0.92	380	2.0		3.0

*H II region

Table 5. (b) Derived nebular parameters for LMC PN.

(1) Name	(2) log F(Hβ) (cgs)	(3) Source for (2)	(4) C(Hβ) Galaxy	(4) C(Hβ) LMC	(5) log I(Hβ) (cgs)	(6) (1+4y)	(7) t	(8) Source for (6) and (7)	(9) $\frac{I(3726)}{I(3729)}$	(10) n_e (cm^{-3})	(11) M(ion) ($M_\odot$)	(12) Optically thick or thin	(13) Predicted ang. diam (arc sec)
LMC N184	-12.67	5	0.16	0.01	-12.50	1.47	1.38	5	1.85	3850	0.29	Thin	0.92
LMC N97	-12.78	4,5,11	0.11	0.07	-12.60	1.68	2.02	11	1.62	2410	0.60	Type I	1.32
LMC N102	-12.74	1,2	0.11	0.05	-12.58	1.66	1.96	5	2.26	8200	0.18	Type I	0.60
LMC N28	-12.84	11	0.09	0.16	-12.59	1.44	1.32	6,11	2.24	7300	0.12	(Type I)	0.56
LMC N110	-12.63	7	0.15	0.02	-12.46	1.49	1.07	7	2.87	1.3×10^4	0.0076	Thick	0.38
LMC N122	-12.54	1	0.13	0.04	-12.37	1.63	1.45	6	1.62	2540	0.69	Type I	1.37
LMC N133	-12.53	7	0.13	0.03	-12.37	1.45	1.15	7	2.88	6.6×10^4	0.019	Thick	0.14
LMC N201	-12.33	1,2	0.11	0.09	-12.13	1.42	1.55	6	2.02	4790	0.59	Thin (Type I)	1.08
LMC N141	-12.48	1	0.11	0.03	-12.34	1.46	1.12	7	2.25	7670	0.17	Thick	0.60
LMC N203	-12.44	1,2	0.15	0.02	-12.27	1.45	0.99	7	2.70	3×10^4	0.046	Thick	0.25
LMC N153	-12.60	1,2,5	0.11	0.06	-12.43	1.53	1.34	5	1.95	4550	0.29	Thin	0.85
LMC N66	-12.68	1	0.09	0.05	-12.54	1.46	1.78	11	1.68	2670	0.48	Thin (Type I)	1.23
LMC N178	-12.68	1,2	0.11	0.10	-12.47	1.46	1.25	5	1.88	3910	0.28	Thin	0.90
LMC LM1-61 (WS 40)	-12.84	4,5	0.11	0.01	-12.72	1.40	1.58	5	1.50	2150	0.34	Thin	1.14

(1) Webster (1969; correction recommended by Webster 1983 applied)
(2) Webster (1976; correction recommended by Webster 1983 applied)
(3) Webster (1983)
(4) Osmer (1976)
(5) Aller (1983)
(6) Monk, Barlow and Clegg (1986)
(7) Barlow and Adams, in preparation
(8) This paper
(9) Aller, Keyes, Ross and O'Mara (1981)
(10) Dufour and Killen (1977)
(11) Barlow, Clegg, Monk and Walker, in preparation

distance moduli of 18.8 and 18.35 mag (Reid & Strugnell 1986). Columns 6 and 7 of Table 5 list the adopted values of $(1+4y)$ and $t[=T_e(\mathrm{O\,III})/10^4\,\mathrm{K}]$, taken from the sources listed in column 8. Column 9 lists the observed $I(3726)/I(3729)$ ratios and column 10 tabulates the electron densities that were derived from these ratios (apart from the exceptions noted below) using the multi-level statistical equilibrium code EQUIB and the O II atomic parameters of Pradhan (1976) and Zeippen (1982). The electron densities were evaluated at $T_e=T_e(\mathrm{O\,III})$, except for the PN labelled 'Type I' in column 12, for which we used the [N II] temperature from the sources listed in column 8. Column 11 tabulates the ionized nebular masses, M(ion), that were derived from equation (5) using the electron densities in column 10.

The [O II] 3726/3729 ratios for SMC N6, N54 and L305 and for LMC N110 and N133 are all at or near the high-density limit. The electron densities listed in column 10 for SMC N6 and for LMC N110 and N133 were derived from their [O II] 7325/3727 ratios (Barlow & Adams, in preparation) while the electron density of $7.4\times10^4\,\mathrm{cm}^{-3}$ listed for SMC N54 was derived from the ratio of [O II] 7325 Å from Aller *et al.* (1981) to [O II] 3727 Å from this paper. The 7325 Å fluxes have not been corrected for the contribution by dielectronic recombination of O^{2+} to this multiplet (see Rubin 1986), with the result that the densities derived from the 7325-3727 ratios may be overestimated. The [S II] 4068 to 6725 Å ratio for SMC N54, from Aller *et al.* (1981), gives $n_e=4\times10^4\,\mathrm{cm}^{-3}$.

The [O II] 3726/3729 ratio found for SMC J2 is close to the low-density limit of 0.67. Near this limit a small change in the [O II] ratio leads to a large change in the derived electron density, so I have preferred to use the observed Hα angular diameter of 2.8 arcsec (Jacoby 1980), in order to derive the electron density using equation (13) below. The resulting electron density of $50\,\mathrm{cm}^{-1}$ (for $\varepsilon=0.5$) gives $I(3726)/I(3729)=0.704$, consistent within the observational errors with the observed ratio of 0.68 (Fig. 1b).

In column 13 of Table 5 the predicted angular diameter, 2θ, is listed for each PN, assuming a simple spherical uniform density distribution. Rearrangement of equation (2) gives

$$2\theta=8.19\times10^6\,t^{0.304}\left[\frac{\gamma I(\mathrm{H}\beta)}{\varepsilon n_e^2 D(\mathrm{kpc})}\right]^{1/3}\ \text{arcsec}, \tag{13}$$

where $\gamma=1+n(\mathrm{He}^+)/n(\mathrm{H}^+)+2n(\mathrm{He}^{2+})/n(\mathrm{H}^+)$. $\varepsilon=0.5$ has been adopted, similar to the filling factor of 0.45 derived for SMC N2 by Barlow *et al.* (1986). Increasing ε to 1.0 would decrease the predicted angular diameters by a factor of 1.26. Since the real density distributions of most PN are likely to be shell-like, the assumption of a uniform density may overestimate the nebular angular diameters. For example, equation (13) predicts an angular diameter of 0.88 arcsec for SMC N2, while the speckle observations of Barlow *et al.* (1986) show that it has two shells, the outermost shell peaking at an angular diameter of 0.76 arcsec, although extending out to at least 0.9 arcsec.

Wood *et al.* (1986) have measured angular diameters by speckle interferometry for six other PN in our sample, with a limit of 0.5 arcsec for the largest diameter measurable by their method. For LMC N122, N201 and N153 they deduced the angular diameters to be larger than this limit, in agreement with the estimates in column 13 of Table 5. For LMC N66 they determined an angular diameter of 0.32 arcsec, substantially less than the predicted diameter of 1.2 arcsec in Table 5. However, Dopita, Ford & Webster (1985) found LMC N66 to show discrete multiple velocity components, implying a lack of spherical symmetry, and concluded that it was 'certainly centrally condensed'. The angular diameter measured by Wood *et al.* may therefore refer only to an inner component. Similarly, Barlow, Marston & Meaburn (in preparation) found LMC LM1−61 (WS 40) to have two velocity components, so again the angular diameter of 0.23 arcsec found by Wood *et al.* may refer only to an inner component. However, SMC N43 was found to show only one velocity component by both Dopita *et al.* (1985) and by Barlow, Marston & Meaburn. Hence,

a different explanation is needed for the discrepancy between the angular diameter of 0.15 arcsec measured by Wood *et al.* (1986) and the predicted diameter of 0.52 arcsec in Table 5.

SMC N8 is a very-low-excitation nebula (Sanduleak & Philip 1977) for which an angular diameter of 3.0 arcsec is predicted in Table 5(a). Henize & Westerlund (1963) noted a possible slightly diffuse Hα image for this nebula, while Sanduleak & Philip noted it as possibly extended in [O II] 3727 Å. The mass of 2.0 $M_\odot$ that is derived for the nebula implies that it is a small H II region, consistent with the Population I status of the central star deduced from its luminosity and effective temperature by Monk, Barlow & Clegg, to be published.

6 Criteria for optical thickness or thinness in the hydrogen Lyman continuum

Planetary nebula envelopes are thought to go through three stages as they expand (Seaton 1966). Initially the nebulae are optically thick in the H I Lyman continuum. During this phase, the ionizing photon luminosity of the central star increases only slowly with time (Schönberner 1981). The nebular ionized hydrogen mass $M(H^+)$ ($\propto n_{H^+}R^3$) is determined by the condition that the number of recombinations ($\propto n_{H^+}n_eR^3$) in the nebula is equal to the number of ionizing photons, which is approximately constant. Hence, as the nebula expands and n_e drops, we obtain $M(H^+)\propto 1/n_e$. The phase is terminated once the entire envelope becomes ionized. During the ensuing optically thin phase, $M(H^+)$ is constant, so the number of recombinations, and thus the Hβ flux, declines linearly with n_e. Eventually the central star, which has been evolving at fairly constant luminosity to higher effective temperatures, begins to decline in luminosity as its nuclear shell-burning sources are extinguished and the star descends along the white dwarf cooling track (Paczynski 1970; Schönberner 1979). At some point the number of ionizing photons emitted by the fading central star may no longer be sufficient to maintain the ionization in the surrounding nebula, which can then enter a final optically thick stage.

The time-scale for a central star of mass M_* to evolve to higher temperatures and then decline in luminosity, is proportional to $M_*^{-9.6}$ (Iben & Renzini 1983), so sufficiently massive central stars may evolve faster than the nebula expands and thereby omit the intermediate optically thin stage of PN evolution, while sufficiently low-mass stars may evolve slowly enough that a final optically thick stage never occurs.

The extreme Type I planetary nebula, defined as having both high He/H and N/O ratios (Peimbert 1978), are believed to be PN excited by relatively high-mass central stars (Peimbert & Torres-Peimbert 1983). The stellar effective temperatures are high enough that the central stars are usually undetectable at optical and ultraviolet wavelengths. Stasinska & Tylenda (1986) have shown that for such objects the usual methods for the determination of central star parameters can break down, thus making it difficult to determine whether the nebulae are thick or thin in the H I Lyman continuum. Column 12 of Table 5 indicates the 10 PN in the sample (four SMC, six LMC) which are classified as Type I because N/O$\geq$0.5, according to the sources listed in column 8. Six have He/H$\geq$0.125 and can therefore be classified as extreme Type I nebulae, according to the criteria of Peimbert & Torres-Peimbert (1983). Each of these nebulae requires a detailed individual analysis before a definitive statement can be made as to whether it is optically thick or thin. The Type I PN probably represent the extreme end of a continuous sequence. Under Peimbert's (1978) original more stringent He/H and N/O classification criteria, SMC L305 would drop out of those listed as fully Type I in Table 5.

One nebula in our sample, LMC N66, has been classified as a Type I PN on a number of grounds (Dopita *et al.* 1985). An ultraviolet and optical spectroscopic study (Barlow *et al.*, in preparation) shows that LMC N66 has N/O=0.53 but that its He/H ratio is not enhanced. It therefore partially qualifies as a Type I PN according to the criteria of Peimbert & Torres-Peimbert (1983) (the same applies to LMC N28). We have classified N66 and N28 as

'(Type I)' to indicate that they do not satisfy the enhanced He criterion for extreme Type I status. The central star continuum of LMC N66 has been detected at *IUE* ultraviolet wavelengths (Barlow *et al.*, in preparation) and a comparison of the Stoy energy balance temperature and He II and H I Zanstra temperatures shows that the nebula is optically thin in the H I Lyman continuum. LMC N66 has therefore been classified as 'thin' in column 12 of Table 5.

Similarly, Barlow *et al.* find that LMC N201 has N/O=0.54 but does not have an enhanced He/H ratio, while the comparison of its Stoy energy balance temperature with its He II and H I Zanstra temperatures show that the nebula is optically thin in the H I Lyman continuum. Therefore LMC N201 has been classified as both 'thin' and '(Type I)' in Table 5.

For the remaining, non-Type I, PN in Table 5, whether they are optically thin or thick in the H I Lyman continuum has been determined either directly from their central star analysis, or on the basis of a more indirect criterion. Harman & Seaton (1966) analysed the central stars of 47 Galactic PN, and concluded that out of 37 PN showing He II 4686 Å emission only six were optically thick in the H I Lyman continuum. Of these six, NGC 6543 and 6572 have Wolf–Rayet-like central stars which contributed the observed He II emission, while of the remaining four PN, NGC 650–1, 6445, 6818 and 6853; all but NGC 6818 have since been classified as Type I (Peimbert & Torres-Peimbert 1983) and are probably in the final optically thick stage of evolution. These three nebulae have been confirmed to be optically thick by Kaler (1983), who derived low luminosities for their central stars.

Among the PN in our sample which show no nebular He II 4686 Å emission, a comparison of ultraviolet H I Zanstra temperatures with Stoy energy balance temperatures (Barlow & Adams, in preparation) shows that SMC N6 and N87 and LMC N110, N133, N141 and N203 are all optically thick in the H I Lyman continuum. They have therefore been classified as 'thick' in column 12 of Table 5 and four other PN which show no He II emission have been similarly classified, namely SMC N38 (Monk *et al.*, to be published) and SMC N43, N54 and N70 (Aller *et al.* 1981); SMC N43 may have extremely weak He II 4686, 0.3 on a Hβ=100 scale). The one exception to this classification rule is SMC L302, which is a very-low-excitation nebula (Sanduleak & Philip 1977) with a WC8 central star (Monk *et al.*, to be published, Barlow & Adams, in preparation). The comparison between its stellar H I Zanstra temperature and Stoy energy balance temperature shows that L302 is optically thin in the H I Lyman continuum. The mass of the central star is low and it would appear that its evolution has been sufficiently slow that the nebula has become optically thin while the central star is still at a relatively low effective temperature.

The remaining PN in the sample all show He II 4686 Å emission. LMC N66 and LMC N201, as previously mentioned, are optically thin in the H I Lyman continuum. Similarly, the nebular modelling of SMC N2 (Barlow *et al.* 1986), shows that it is optically thin in the H I Lyman continuum.

These results support the conclusion of Harman & Seaton (1966) that almost all PN which show He II 4686 Å emission are optically thin in the H I Lyman continuum and so all such non-Type I nebulae have been classified as 'thin' in column 12 of Table 5. It should, however, be borne in mind that exceptions may occur for sufficiently massive central stars, and so a central star analysis is desirable for each PN. For example, NGC 7027 shows strong He II 4686 but is optically thick in H I and is believed to be powered by a rapidly evolving high-mass central star [see Tylenda (1984), who has proposed that NGC 7027 is in the final optically thick phase]. Similarly, NGC 3918 shows strong He II 4686, contains optically thick zones, and has a high-luminosity central star (Clegg *et al.* 1986).

Ten of the PN in the sample have thus been classified as optically thin or thick directly on the basis of their central star analyses, while a further 14 have been classified on the basis of the presence or absence of nebular He II 4686 in their spectra. Inspection of columns 10 and 12 of

Table 5 reveals the remarkable result that all of the PN classified as optically thin have $n_e<5000\,cm^{-3}$, while all of those classified as optically thick have $n_e>6000\,cm^{-3}$. It would therefore appear that for the 'average' PN the transition from the optically thick to optically thin phase occurs at an electron density of 5000–6000 cm^{-3}. If one makes the assumption that the Hβ fluxes of the optically thick PN remain relatively constant until the moment they become optically thin, then the use of $n_e=5000$–$6000\,cm^{-3}$ in equation (5) predicts masses similar to those found for the nebula classified as optically thin.

The 10 PN in the sample which are classified as optically thick show a range of only a factor of 1.8 in their intrinsic Hβ fluxes. Their mean dereddened Hβ flux is equivalent to $\log I(H\beta)=-12.48\pm0.09$ at the distance of the SMC. Apart from SMC N44, all of the non-Type I PN classified as optically thin have significantly lower Hβ fluxes than this, as would be expected for nebulae whose fluxes should decline as n_e once they become optically thin. SMC N44 has weak He II 4686 [$\sim0.01\,I(H\beta)$, Aller *et al.* 1981] and has the highest electron density (4620 cm^{-3}) of any of the 12 'normal' PN classified as optically thin in the sample (see Section 7). The fact that its Hβ flux is comparable to those of the optically thick PN, while its ionized mass is comparable to those of the optically thin PN, suggests that it is in transition between the two groups.

Pottasch (1983), using his own distance scale for Galactic PN, found that his derived nebular masses increased inversely with declining electron density until $n_e\sim300\,cm^{-3}$ was reached, and argued that PN do not become optically thin until their densities drop to this value. However, the present results for Magellanic Cloud PN do not support this argument, since among the SMC PN which have been classified as optically thin, the three with $n_e<2000\,cm^{-3}$ have the same mean mass as the three with $n_e>3800\,cm^{-3}$. If the comparison with the results of Pottasch is confined to Galactic Centre PN only, for which the distances are more reliable, then better agreement is obtained with the present results.

Of the 14 PN classified as optically thin in Table 5, all but one have electron densities between 900 and 5000 cm^{-3}, which, as discussed in Section 3, is the density range of highest reliability for the derivation of nebular masses using the [O II] 3726, 3729 ratio.

All of the Type I PN in the sample show strong He II 4686 emission. Since LMC N102 and N28 have $n_e\sim8000\,cm^{-3}$, they clearly do not obey the same relationship between electron density and the presence of He II as the non-Type I PN. Presumably the more massive central stars in Type I PN evolve to high effective temperatures while the nebula are at higher densities than the 'average' PN. The ionized masses derived for LMC N102 and N28 are significantly less than for the lower density LMC Type I nebulae, N97 and N122. This may be interpreted as implying that N102 and N28 are still optically thick in H I. The ionized masses derived for N97 and N122 are high, 0.60 and 0.69 $M_\odot$, respectively, so it is possible that they are optically thin. Similarly, SMC N67 and L536 have high ionized masses, 0.45 and 0.40 $M_\odot$, respectively, and these two Type I PN may also be optically thin. The [O II] emission from SMC L305 appears to be dominated by a high-density core.

The ionized mass of 0.19 $M_\odot$ listed in Table 5 for SMC J2 was derived from its Hβ flux (Barlow *et al.*, in preparation) and its observed angular diameter of 2.8 arcsec (Jacoby 1980), assuming $\varepsilon=0.5$ (a filling factor of 1.0 would give an ionized mass of 0.24 $M_\odot$). This is significantly less than the ionized mass of 0.72 $M_\odot$ that was derived by Jacoby (1980) under the assumption that the observed red magnitude was almost entirely due to Hα. The spectra of Barlow *et al.* show that 75 per cent of the red flux is due to [N II] 6548, 6584 Å. In addition, the distance adopted here for the SMC is a factor of 1.2 smaller than that adopted by Jacoby. Barlow *et al.* derive N/O=0.7 for SMC J2, which meets one of the conditions for Type I status (Peimbert & Torres-Peimbert 1983). Its Hβ flux is 200 times fainter than that of the brightest SMC PN and the presence of very strong lines of [O II] and [N II], as well as strong He II 4686, implies that it is in the final optically thick phase. Its ionized mass of 0.19 $M_\odot$ is likely to be significantly less than the total nebular mass.

SMC J2 appears to be very similar to the low-density Galactic PN NGC 6853 and 7293 which are both optically thick (Bohlin, Harrington & Stecher 1982) and which can both be classified as Type I PN (Peimbert & Torres-Peimbert 1983; Hawley 1978).

7 Discussion: implications for the planetary nebula distance scale

Wood, Bessell & Fox (1983) have predicted that the nebular masses of PN should show a steep dependence upon central star mass. The present results appear to confirm this. Table 5 shows that the highest nebular masses in each cloud belong to Type I PN (N67 and L536 in the SMC and N97, N122, N201 and N66 in the LMC), nebulae which are believed to have relatively high-mass central stars (see Peimbert & Torres-Peimbert 1983). If planetary nebula central stars have a flat mass distribution, then the results of Wood *et al.* (1983) would imply that a very large range in nebular masses should be encountered.

However, Schönberner (1981) and Schönberner & Weidemann (1983) have argued that, although high-mass nuclei do exist, the mass distribution of planetary nebula central stars is very highly peaked around $\sim 0.58\,M_{\odot}$ and similar to that of DA white dwarfs. If correct, this should have the consequence that the masses of most planetary nebula envelopes should also lie within a fairly narrow range. This is also required for self-consistency, since the results of Schönberner & Weidemann are based upon distances using the Shlovsky method, which assumes that all optically thin PN have the same ionized nebular mass.

Most applications of the Shlovsky method to Galactic PN (e.g. O'Dell 1962; Seaton 1968; Cahn & Kaler 1971) have utilized nebular angular radii and Balmer line fluxes in order to derive distances. If one assumes a uniform spherically symmetric planetary nebula, then from equations (1) and (2) one obtains

$$D^5=\frac{3\gamma h\nu_{\beta}\alpha_{\rm eff}(\mathrm{H}\beta)M_{\rm H}^2}{(4\pi)^2\varepsilon\theta^3 m_{\rm H}^2 I(\mathrm{H}\beta)}, \tag{14}$$

where $\gamma=n_{\rm e}/n(\mathrm{H}^+)$, θ is the nebular angular radius, $M_{\rm H}$ is the ionized hydrogen mass of the nebula and $m_{\rm H}$ is the mass of a hydrogen atom. Evaluation of (14) gives

$$D(\mathrm{kpc})=0.160\left[\frac{\gamma M_{\rm H}^2 t^{-0.913}}{\varepsilon\theta^3 I(\mathrm{H}\beta)}\right]^{1/5}, \tag{15}$$

where $M_{\rm H}$ is in $M_{\odot}$, θ is in arcsec, $I(\mathrm{H}\beta)$ is in erg cm^{-2} s^{-1}, and $t=T_{\rm e}/10^4$ K.

Excluding Type I PN, the 12 optically thin PN in the sample give $M_{\rm H}=0.189\pm0.043\,M_{\odot}$ [$M(\mathrm{ion})=0.27\pm M_{\odot}$]. The total range in $M_{\rm H}$ for these 12 PN is a factor of 2, which translates into an uncertainty in the derived distance D of ± 15 per cent, from equation (15), which is sufficiently small for the Shlovsky method to be applicable. If one substitutes the mean value of $M_{\rm H}=0.189\,M_{\odot}$ and adopts $\varepsilon=0.65$, the preferred value of ε of Seaton (1968) and of Cahn & Kaler (1971), one obtains

$$\begin{aligned} D(\mathrm{kpc}) &= 8.96\times10^{-2}\gamma^{1/5}\theta^{-3/5}I^{-1/5}(\mathrm{H}\beta)t^{-0.183} \\ &= 8.76\times10^{-2}\theta^{-3/5}I^{-1/5}(\mathrm{H}\beta), \end{aligned} \tag{16}$$

for $t=1.29$ and $\gamma=1.13$, the mean values for the optically thin PN. Shlovsky (1956) and O'Dell (1962) derived values for the normalizing constant in equation (16) which in each case were based mainly upon observations of a few nearby Galactic PN. For the same values of ε, γ and t as above, the normalizing constant of Shlovsky (1956) is equivalent to $M_{\rm H}=0.14\,M_{\odot}$, while that of O'Dell (1962) is equivalent to $M_{\rm H}=0.126\,M_{\odot}$. Seaton (1968) derived the value of the normalizing

constant in equation (16) from the assumption that the Galactic PN with the highest Hβ surface brightnesses corresponded to the Magellanic Cloud PN in Webster's (1969) sample which had the highest Hβ luminosities. For the same parameters as above, the normalizing constant of Seaton (1968) used, by Cahn & Kaler (1971), is equivalent to $M_{\rm H}=0.131\,M_{\odot}$. The larger value of $M_{\rm H}=0.189\,M_{\odot}$ derived here is therefore, by equation (15), eqivalent to a 16 per cent increase in the Seaton/Cahn & Kaler (CK) distance scale. However, it should be noted that most CK distances derived from Balmer line fluxes need to be corrected further, to allow for the overestimation of extinction at Hβ by the CK Galactic dust distribution model. A comparison of the CK extinctions, for PN with Hβ fluxes, with the individual radio–Hβ method extinctions derived by Milne & Aller (1975; 94 PN in common), shows that the CK extinctions are too large by an average of 0.45 dex. A similar comparison with the individual extinctions listed by Shaw & Kaler (1985; 31 PN in common), shows the CK extinctions to be too large by a mean of 0.41 dex. While the CK distances should be corrected individually, one would expect, by (16), that the overall CK distances should increase by an average of 22 per cent once the extinction corrections are applied. The combination of the corrections for (i) increased nebular mass and (ii) decreased extinction, should thus lead to an average increase in the CK distances of 41 per cent.

For comparison, Cudworth (1974) derived distances for Galactic PN from statistical parallaxes which, for the 39 PN classified as optically thin by Cudworth, are an average of 58 per cent larger than those of Cahn & Kaler (1971), so distances derived for optically thin PN from equation (16) should be on average 12 per cent lower than those of Cudworth.

Weidemann (1977) and Schönberner (1981) adopted PN distances which were 30 per cent larger than those of CK. The PN distance scale of Maciel (1984) is 20 per cent larger than that of CK. Therefore distances for optically thin PN derived using equation (16) should be only 8 per cent larger, on average, than those of Weidemann and Schönberner and 17 per cent larger than those of Maciel. Finally, equation (16) will give PN distances which are on average 69 per cent larger than those of Acker (1978).

The angular radii of PN can be difficult to measure accurately for small distant nebulae or for nebulae which exhibit a large range in surface brightness. An alternative method of distance estimation for optically thin PN, using the [O II] doublet ratio, therefore suggests itself. From equation (5) one has

$$D(\mathrm{kpc})=1.11\times10^{-6}[M_{\rm H}n_{\rm e}(\mathrm{O\,II})/I(\mathrm{H}\beta)]^{1/2}t^{-0.457}$$
$$=4.82\times10^{-7}[n_{\rm e}(\mathrm{O\,II})/I(\mathrm{H}\beta)]^{1/2}t^{-0.457}\qquad \text{for } M_{\rm H}=0.189\,M_{\odot}. \tag{17}$$

This method of distance estimation has the advantage that $n_{\rm e}$(O II), the electron density derived from the integrated nebular [O II] 3726, 3729 Å doublet ratio, is a direct mass tracer, as shown in Section 3, so the assumption of a uniform spherically symmetric nebular structure is not being made, nor is a filling factor being assumed. Since the method requires that $n_{\rm e}$(O II) be the value appropriate for the entire nebula, large-aperture measurements of the [O II] doublet ratio would be required for most Galactic PN, e.g. using Fabry–Perot interferometers.

The application of equation (17) to the least massive optically thin PN in the sample (SMC N4) leads to an overestimate by 24 per cent of the adopted SMC distance of 57.5 kpc, while application to the most massive PN in the group (SMC N2) underestimates the adopted SMC distance by 15 per cent. These errors are of the same order as the uncertainty in the mean distances of the Magellanic Clouds themselves (see Reid & Strugnell 1986). Mathewson, Ford & Visvanathan (1986) have in fact proposed that the SMC is strung out over a considerable depth.

For optically thick PN, one can determine distances by a method first utilized by Zanstra (1931) and Vorontsov-Velyaminov (1934), based on the assumption that all optically thick PN have the same absolute magnitude. For the 10 PN classified as optically thick in Table 5, the total range in

intrinsic Hβ flux is only a factor of 1.8, sufficiently small for the method to be useful. The mean dereddened Hβ fluxes of thse 10 PN correspond to $\log I(\mathrm{H}\beta) = -8.96 \pm 0.09$ at a distance of 1 kpc. For optically thick PN, one therefore has

$$D(\mathrm{kpc}) = 3.32 \times 10^{-5} I^{-1/2}(\mathrm{H}\beta). \quad (18)$$

This calibration agrees almost exactly with that obtained by O'Dell (1963) for optically thick Galactic PN, $\log I(\mathrm{H}\beta) = -9.0 \pm 0.1$ at 1 kpc, and gives distances that are larger by a factor of 1.88 than those that would be obtained with the lower absolute Hβ flux calibration of Cudworth (1974) for optically thick PN. Equation (18) overestimates by 20 per cent the distance to LMC N110, the optically thick PN with the lowest Hβ luminosity in the sample, while it underestimates by 11 per cent the distance to SMC N54, the PN with the highest Hβ luminosity. Equation (18) should not be used to estimate the distances to very-low-excitation (VLE) planetary nebulae, since the low effective temperature central stars of such PN are likely to emit significantly fewer ionizing photons than the plateau value attained at higher effective temperatures (see fig. 6 of Schönberner 1981).

On the basis of our present results, the distances to non-type I PN which show nebular He II 4686 Å emission and which have $n_e(\mathrm{O\,II}) < 5000\,\mathrm{cm}^{-3}$ should be determined using equations (16) or (17), while the distances to PN which show no nebular He II emission and which have $n_e > 6000\,\mathrm{cm}^{-3}$ should be determined using equation (18). As pointed out by Minkowski (1965), the application of either the optically thin method or the optically thick method to an inappropriate PN will lead to an overestimate for the distance, and so the lower of the distances derived by each method should be preferred.

If, following the discussion in Section 6, one was to more speculatively assume that all six of the Type I PN in the sample with $500\,\mathrm{cm}^{-3} < n_e < 5000\,\mathrm{cm}^{-3}$ are predominantly ionized, then their mean hydrogen mass is $0.33 \pm 0.08\,M_\odot$ and their range in hydrogen mass is a factor of 2 (the four LMC Type I PN with $n_e \leqslant 5000\,\mathrm{cm}^{-3}$ give $M_\mathrm{H} = 0.38 \pm 0.05\,M_\odot$). This might allow one to estimate the distances of similarly low-density Galactic Type I PN by the Shlovsky method, using equations (16) or (17) with $M_\mathrm{H} = 0.33\,M_\odot$.

The current results are based upon a sample of 12 non-Type I PN classified as optically thin and 10 classified as optically thick. A larger sample of Magellanic Cloud PN is desirable in order that the statistical base be broadened. Such a sample should allow one to determine whether any optically thick PN exist at significantly lower intrinsic Hβ flux levels than encountered here. Optically thin PN with lower masses than encountered in the present sample could also possibly be present at fainter Hβ flux levels. However, the intrinsic Hβ fluxes of the non-Type I PN which are classified as optically thin in the current sample already cover a range of over a factor of 20 and the derived hydrogen masses of the four brightest and four faintest are very similar, 0.21 ± 0.03 and $0.19 \pm 0.05\,M_\odot$, respectively.

Acknowledgments

The observations presented in this paper were obtained during a PATT allocation of time on the Anglo–Australian Telescope, and through PATT SERC Service Observations on the AAT. I am grateful to Drs J. R. Walsh, D. C. Morton and J. G. Robertson for obtaining the 1985 AAT Service spectra. I am also grateful to Drs J. R. Walsh and J. B. Kaler for their comments on the manuscript. I thank David Monk for his assistance with the DIPSO analysis at the UCL STARLINK node and Steven Voels for his help with the use of the IRAF package on the JILA VAX 8600. IRAF is distributed by the National Optical Astronomy Observatories, which is operated by AURA, Inc., under contract to the US National Science Foundation.

References

Acker, A., 1978. *Astr. Astrophys. Suppl.*, **33,** 367.
Aller, L. H., 1983. *Astrophys. J.*, **273,** 590.
Aller, L. H., Keyes, C. D., Ross, J. E. & O'Mara, B. J., 1981. *Mon. Not. R. astr. Soc.*, **194,** 613.
Barlow, M. J., Morgan, B. L., Standley, C. & Vine, H., 1986. *Mon. Not. R. astr. Soc.*, **223,** 151.
Bohlin, R. C., Harrington, J. P. & Stecher, T. P., 1982. *Astrophys. J.*, **252,** 635.
Brocklehurst, M., 1971. *Mon. Not. R. astr. Soc.*, **153,** 471.
Burstein, D. & Heiles, C., 1982. *Astr. J.*, **87,** 1165.
Cahn, J. H. & Kaler, J. B., 1971. *Astrophys. J. Suppl.*, **22,** 319.
Clegg, R. E. S., Harrington, J. P., Barlow, M. J. & Walsh, J. R., 1987. *Astrophys. J.*, **314,** 551.
Cudworth, K. M., 1974. *Astr. J.*, **79,** 1384.
Dopita, M. A., Ford, H. C. & Webster, B. L., 1985. *Astrophys. J.*, **297,** 593.
Dopita, M. A., Ford, H. C., Lawrence, C. J. & Webster, B. L., 1985. *Astrophys. J.*, **296,** 390.
Dufour, R. J. & Killen, R. M., 1977. *Astrophys. J.*, **211,** 68.
Fitzpatrick, E. L., 1985. *Astrophys. J. Suppl.*, **59,** 77.
Harman, R. J. & Seaton, M. J., 1966. *Mon. Not. R. astr. Soc.*, **132,** 15.
Harrington, J. P. & Feibelman, W. A., 1983. *Astrophys. J.*, **265,** 258.
Harrington, J. P., Seaton, M. J., Adams, S. & Lutz, J. H., 1982. *Mon. Not. R. astr. Soc.*, **199,** 517.
Hawley, S. A., 1978. *Publs astr. Soc Pacif.*, **90,** 370.
Henize, K. G., 1956. *Astrophys. J. Suppl.*, **2,** 315.
Henize, K. G. & Westerlund, B. E., 1963. *Astrophys. J.*, **137,** 747.
Hindman, J. V., 1967. *Aust. J. Phys.*, **20,** 147.
Howarth, I. D., 1983. *Mon. Not. R. astr. Soc.*, **203,** 301.
Howarth, I. D. & Maslen, D. M., 1984. *Starlink User Note 50.*
Iben, I., Jr & Renzini, A., 1983. *Ann. Rev. Astr. Astrophys.*, **21,** 271.
Jacoby, G. H., 1980. *Astrophys. J. Suppl.*, **42,** 1.
Kaler, J. B., 1981. *Astrophys. J.*, **250,** L31.
Kaler, J. B., 1983. *Astrophys. J.*, **271,** 188.
Koornneef, J., 1982. *Astr. Astrophys.*, **107,** 247.
Lindsay, E. M., 1961. *Astr. J.*, **66,** 169.
Lindsay, E. M. & Mullan, D. J., 1963. *Irish Astr. J.*, **6,** 51.
Maciel, W. J., 1984. *Astr. Astrophys. Suppl.*, **55,** 253.
Mathewson, D. S., Ford, V. L. & Visvanathan, N., 1986. *Astrophys. J.*, **301,** 664.
Mendoza, C., 1983. In: *Planetary Nebula, IAU Symp. No. 103,* p. 143, ed. Flower, D. R., Reidel, Dordrecht, Holland.
Milne, D. K. & Aller, L. H., 1975. *Astr. Astrophys.*, **38,** 183.
Minkowski, R., 1965. In: *Galactic Structure,* p. 321, eds Blaauw, A. & Schmidt, M., University of Chicago Press.
O'Dell, C. R., 1962. *Astrophys. J.*, **135,** 371.
O'Dell, C. R., 1963. *Astrophys. J.*, **138,** 67.
Oke, J. B., 1974. *Astrophys. J. Suppl.*, **27,** 21.
Osmer, P. S., 1976. *Astrophys. J.*, **203,** 352.
Osterbrock, D. E., 1974. *Astrophysics of Gaseous Nebula,* p. 53, W. H. Freeman, San Francisco.
Paczynski, B., 1970. *Acta Astr.*, **20,** 47.
Peimbert, M., 1978. In: *Planetary Nebulae, IAU Symp. No. 76,* p. 215, ed. Terzian, Y., Reidel, Dordrecht, Holland.
Peimbert, M. & Torres-Peimbert, S., 1983. In: *Planetary Nebulae, IAU Symp No. 103*, p. 233, ed. Flower, D. R., Reidel, Dordrecht, Holland.
Pottasch, S. R., 1983. In: *Planetary Nebulae, IAU Symp. No. 103*, p. 391, ed. Flower, D. R., Reidel, Dordrecht, Holland.
Pradhan, A. K., 1976. *Mon. Not. R. astr. Soc.*, **177,** 31.
Reid, I. N. & Strugnell, P. R., 1986. *Mon. Not. R. astr. Soc.*, **221,** 887.
Rohlfs, K., Kreitschmann, J., Siegman, B. C. & Feitzinger, J. V., 1984. *Astr. Astrophys.*, **137,** 343.
Rubin, R. H., 1986. *Astrophys. J.*, **309,** 334.
Sanduleak, N., MacConnell, D. J. & Philip, A. G. D., 1978. *Publs astr. Soc. Pacif.*, **90,** 621.
Sanduleak, N. & Philip, A. G. D., 1977. *Publs astr. Soc. Pacif.*, **89,** 792.
Schönberner, D., 1979. *Astr. Astrophys.*, **79,** 108.
Schönberner, D., 1981. *Astr. Astrophys.*, **103,** 119.
Schönberner, D. & Weidemann, V., 1983. In: *Planetary Nebulae, IAU Symp. No. 103,* p. 359, ed. Flower, D. R., Reidel, Dordrecht, Holland.

Seaton, M. J., 1966. *Mon. Not. R. astr. Soc.,* **132,** 113.
Seaton, M. J., 1968. *Astrophys. Lett.,* **2,** 55.
Shames, P. M. B & Tody, D., 1986. *Draft IRAF CL User Guide.*
Shaw, R. A. & Kaler, J. B., 1985. *Astrophys. J.,* **295,** 537.
Shlovsky, I. S., 1956, *Astr. Zh.,* **33,** 222.
Stasinska, G. & Tylenda, R., 1986. *Astr. Astrophys.,* **155,** 137.
Tylenda, R., 1984. *Astr. Astrophys.,* **138,** 317.
Vorontsov-Velyaminov, B. A., 1934. *Z. Astrophys.,* **8,** 195.
Webster, B. L., 1969. *Mon. Not. R. astr. Soc.,* **143,** 79.
Webster, B. L., 1976. *Mon. Not. R. astr. Soc.,* **174,** 513.
Webster, B. L., 1983. *Publs astr. Soc. Pacif.,* **95,** 610.
Weidemann, V., 1977. *Astr. Astrophys.,* **59,** 411.
Wood, P. R., Bessell, M. S. & Dopita, M. A., 1986. *Astrophys. J.,* **311,** 632.
Wood, P. R., Bessell, M. S. & Fox, M. W., 1983. *Astrophys. J.,* **272,** 99.
Zanstra, H., 1931. *Z. Astrophys.,* **2,** 329.
Zeippen, C. J., 1982. *Mon. Not. R. astr. Soc.,* **198,** 111.